Am J Transl Res 2021;13(11):13043-13050
www.ajtr.org /ISSN:1943-8141/AJTR0106925

Original Article

Effect of astaxanthin on neuron damage, inflammatory factors expressions and oxidative stress in mice with subarachnoid hemorrhage

Yu Qian[1,2*], Xinyu Lu[2*], Lulu Chen[3], Jinyu Sun[3], Kan Cao[2], Qiang Yu[2], Junfei Shao[1]

[1]Department of Neurosurgery, Nanjing Medical University Affiliated Wuxi People's Hospital, Wuxi 214023, Jiangsu Province, China; [2]Department of Neurosurgery, Jiangsu University Affiliated People's Hospital, Zhenjiang 212000, Jiangsu Province, China; [3]Department of Anatomy, Histology and Embryology, Nanjing Medical University, Nanjing 211166, Jiangsu Province, China. [*]Equal contributors and co-first authors.

Received December 24, 2019; Accepted January 15, 2020; Epub November 15, 2021; Published November 30, 2021

Abstract: Objective: This study aimed to explore the effect of astaxanthin (ATX) on neuron damage, inflammatory factor expression and oxidative stress in mice with subarachnoid hemorrhage (SAH). Methods: Specific-pathogen-free, 'Institute of Cancer Research', male mice were randomly divided into four groups: SAH group, sham group, SAH + placebo group (SAH + Vehicle group) and SAH + ATX group. Neurological function was scored in each group. Brain water content, reactive oxygen species (ROS) content and inflammatory factor levels in the brain were detected by wet-dry weighting method, DCFH-DA fluorescent probe staining method and ELISA, respectively. Expression of NADPH oxidase 2 (NOX2), glial fibrillary acidic protein (GFAP) and apoptosis-related proteins Bax and Bcl-2 were detected by Western blot and quantitative real-time polymerase chain reaction. Neuronal apoptosis was detected by TUNEL staining. Results: Compared with sham group, neurological score, brain water content and ROS content in the other three groups increased significantly (all $P<0.05$). Neurological score, brain water content and ROS content in SAH + ATX group were lower than those in SAH group (all $P<0.05$). Compared with the sham group, there was increased expression of interleukin (IL)-6, IL-17 and tumor necrosis factor α (TNF-α), and increased neuronal apoptosis, as well as enhanced expression of NOX2, GFAP and Bax; while there was decreased IL-10 expression, and declined Bcl-2 expression, in the other three groups (all $P<0.05$). There was decreased expression of IL-6, IL-17 and TNF-α, declined expressions of NOX2, GFAP and Bax, and lowered neuronal apoptosis; while there was increased IL-10 expression, and enhanced Bcl-2 expression, in SAH + ATX group as compared to SAH group (all $P<0.05$). All indicators between SAH group and SAH + Vehicle group showed no significant differences (all $P>0.05$). Conclusion: Astaxanthin can decrease neuron damage, inhibit inflammatory response, and improve oxidative stress in SAH mice. Thus, astaxanthin is a method for treating SAH.

Keywords: Astaxanthin, subarachnoid hemorrhage, neuron damage, inflammatory factor, oxidative stress

Introduction

Subarachnoid hemorrhage (SAH) refers to the condition where blood flows into the subarachnoid space after intracranial vascular rupture [1, 2]. Traumatic and non-traumatic SAH are two common conditions of SAH, and SAH has been a common disease with an extremely high mortality rate [3]. Although the diagnostic method, intravascular intervention and perioperative nursing have obtained great progression, the prognosis for SAH patients after treatment is still poor [4, 5]. Early brain injury may be the primary factor causing SAH patient death as well as affecting the prognosis [6]. Increased intracranial pressure, blood-brain barrier disruption, inflammatory response enhancement, brain edema and neuron death are all manifestations of early brain injury [7, 8].

Astaxanthin (ATX) is a type of keto form carotenoids and an antioxidant drug derived from marine organisms, fungi and a small amount of plants [9-11]. ATX has been proved having multiple biological functions, such as neuroprotection, anti-inflammatory abilities, anti-apoptosis and antioxidant actions, and can improve immune function [12-14]. Basic research has con-

firmed that ATX significantly alleviates oxidative damage in the treatment of cerebral infarction, myocardial ischemia reperfusion injury, and other cardiovascular diseases [15, 16]. ATX has been found to have a significant neuroprotective effect after the occurrence of SAH [17]. However, the specific mechanism of ATX regulating SAH still needs further exploration. In this study, SAH model mice were established and treated with ATX in order to explore the effect of ATX on neuronal apoptosis, inflammatory factor expression and oxidative stress in SAH mice.

Materials and methods

Establishment of the SAH mouse model

Fifty specific-pathogen-free healthy adult male mice (purchased from the Animal Research Center of Jiangsu University) weighing 28-32 g at 8-10 weeks old were housed in a clean environment with 12 h of light and free accessed to water. Then SAH mice models were constructed. Mice were first anesthetized by intraperitoneally injecting 0.3 mL/kg chloral hydrate (10%). Mice were fixed on the stereotaxic apparatus in a prone position after shaving parietal fur. Skin preparation on the apex was performed, and the field of operation was disinfected routinely with povidone iodine. Then the skin of about 3 cm was incised along the sagittal line at the midpoint of the calvarium. The muscle and subcutaneous soft tissue were separated to fully expose the atlanto-occipital membrane. The tip of a polyethylene catheter was inserted into the atlanto-occipital membrane for 10 mm. The bone hole was closed by bone wax. Clear cerebrospinal fluid could be seen after the syringe was connected to the catheter and pumped back. Then mice were shifted to the supine position. The skin of inner thigh was incised to separate the femoral arteries. Then 0.2 mL arterial blood was drawn and injected into the subarachnoid space through the polyethylene catheter at a speed of 0.1 mL/min. The catheter was removed. The bone hole was closed. The incision was sutured and disinfected, and the mice were kept in a head-down position for 30 min. Then their heads were raised and they were observed in the feeding box. Mice in the sham group were also treated by the above methods, except that no autologous arterial blood was injected after subarachnoid space catheterization. This study was approved by the Animal Experiment Ethics Committee of Jiangsu University Affiliated People's Hospital, and the animal use and experiment operations were in accordance with the regulations of Jiangsu University for experimental animals.

Animal grouping

Mice were divided into four groups by using a random number table, with 10 mice in each group: SAH group, sham group, SAH + placebo group (SAH + Vehicle group) and SAH + ATX group. In the SAH + Vehicle group, 10% dimethyl sulfoxide (DMSO) and normal saline mixture of 10 μL were injected into the lateral ventricle of mice at 30 min after SAH. In the SAH + ATX group, 0.1 mmol/L ATX (Product number A-3236, Sigma, USA) was dissolved in 10% DMSO and injected into the lateral ventricle of mice at 30 min after SAH. The injection dose of DMSO and ATX was 100 mg/kg based on the body weight of mice.

Neurological function scoring

Longa 5-grade scoring method was used to score the neurological function of mice at 48 h after the surgery [18]. No obvious neurological impairment symptom was scored as 0; the condition when the bilateral fore limbs of the mouse flexed and could not be straightened after hemorrhage was scored as 1; the symptom of circling was scored as 2; when hemiplegia and toppling occurred during walking, this was scored as 3; total difficulty in walking and loss of consciousness was scored as 4. Scores 1-3 represented successful modeling.

Brain water content detected by wet-dry weighting method

After neurological function scoring, mice were killed by intraperitoneally injecting pentobarbital sodium solution (200 mg/kg). The brain tissue of mice was removed and preserved. The blood was sucked dry by using filter paper, and the wet weight of the brain tissue was weighed on an electronic balance. The dry weight was weighed after brain tissue was dried in a drying oven at 80°C for 72 h. Brain water content = (wet weight-dry weight)/wet weight * 100%.

Reactive oxygen species detection

The cryopreserved brain tissue was put into pre-cooled homogenate buffer at a ratio of 1:10 and ground on ice. Then the brain tissue homogenate was mixed with 10 μmol/L DCFH-

Table 1. Primer sequence

Gene	Primer sequence (5'-3')	
	Forward	Reverse
NOX2	CACGAACCTAGAATCGACC	ATGTTACCACCTGTCTCGCG
GFAP	CGGGAGTCACCCAACTCTG	TGGGAGATTCGTCAGAGACAA
Bax	CTGAGCGATGGACTCTGC	GACCCCTCAAAGACGAATG
Bcl-2	GAAAGTCATGAGACCCGTCC	GTGGTACAACTCGCATCAAG
GAPDH	ACCAGTGCCTCCACAATCAC	CACTTGCTCCACCTGCTGTA

Note: NOX2: NADPH oxidase 2; GFAP: glial fibrillary acidic protein.

DA fluorescent probe (BB-47053, Shanghai BestBio Science Co. Ltd., China) and incubated at 37°C for 20 min. The homogenate was rinsed with phosphate buffered saline three times. Fluorescence intensity of dichlorofluorescein was detected by a fluorescence microplate reader with an excitation wavelength of 502 nm and an emission wavelength of 530 nm to obtain the level of reactive oxygen species (ROS).

Inflammatory factor levels in brain tissue detected by ELISA

The cryopreserved brain tissue was put into pre-cooled homogenate buffer at a ratio of 1:10 and ground on ice. The levels of interleukin (IL)-6, IL-10, IL-17 and tumor necrosis factor α (TNF-α) were determined according to the instructions of corresponding kits (IL-6, IL-10, and IL-17: EK0411, EK0417, EK0796, Boster Biological Technology Co. Ltd., Wuhan, China; TNF-α: D720008-0048, Sangon Biotech (Shanghai) Co. Ltd., China). Optical density at 450nm was detected by a microplate reader to calculate the level of inflammatory factors.

Quantitative real-time polymerase chain reaction test

RNA extraction kit (R1200-50T, Beijing Solarbio Science & Technology Co. Ltd., China) was used to extract total RNA in brain tissue. RNA was reversely transcribed into cDNA by using reverse a transcription kit (RP1200, Beijing Solarbio Science & Technology Co. Ltd., China). The reaction conditions and reaction system were performed according to the kit instructions. The primers of NADPH oxidase 2 (NOX2), glial fibrillary acidic protein (GFAP), Bax and Bcl-2 were synthesized by the Shanghai Genechem Co. Ltd., China (**Table 1**). All factors used GAPDH as the internal reference. The expression of related factors was calculated by the $2^{-\Delta\Delta Ct}$ method. ΔΔCt = (mean CT value of target gene in experimental group-mean CT value of housekeeping gene in experimental group)-(mean CT value of target gene in control group-mean CT value of housekeeping gene in control group).

Western blot test

The brain tissue was lysed in RIPA protein lysis buffer (P0013B, Beyotime Institute of Biotechnology, China) was placed on ice for 30 min and centrifuged at 12,000 r/min for 10 min. Total protein content was measured according to the instruction of BCA kit (P0012S, Beyotime Institute of Biotechnology, China). Protein was quantified based on different concentrations, separated by polyacrylamide gel electrophoresis and transferred to a PVDF membrane by wet transfer method. The membrane was sealed in TRIS buffered saline tween buffer solution containing 10% skim milk powder at room temperature for 1 h. Then the membrane was incubated with primary antibodies; rabbit anti-mouse NOX2 (1:5000, ab129068, ABCAM, UK), GFAP (0.1 μg/mL, ab53554, ABCAM, UK), Bax (1:2000, ab18-2733, ABCAM, UK), and Bcl-2 (1:2000, ab18-2858, ABCAM, UK) overnight. After being rinsed with phosphate buffered saline tween (PBST), the membrane was incubated with horseradish peroxidase-labeled secondary antibody goat anti-rabbit IgG (1:20000, ab205718, ABCAM, UK) at room temperature for 1 h. The membrane was rinsed with PBST, and its color was developed by enhanced chemiluminescence. The test results were semi-quantified by Image J software to calculate the relative expression level of protein. Relative expression level of protein = gray value of target band/gray value of internal reference band.

Neuronal apoptosis was detection by the TUNEL method

Neuronal apoptosis was detected by TUNEL staining by referring to the instruction of the *in situ* cell apoptosis detection kit (116848099-10, Roche, Switzerland). The brain tissue was sectioned, dewaxed, and hydrated, followed by repairing with citric acid-sodium citrate solution for 10 min. TUNEL reaction solution (enzyme solution: label solution = 1:9) was prepared. Each slice was incubated in 50 μL TUNEL reac-

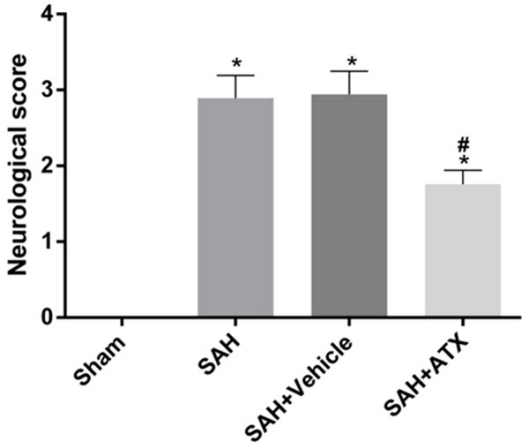

Figure 1. Neurological score in each group. Compared with sham group, *P<0.05; compared with SAH group, #P<0.05. ATX: astaxanthin; SAH: subarachnoid hemorrhage.

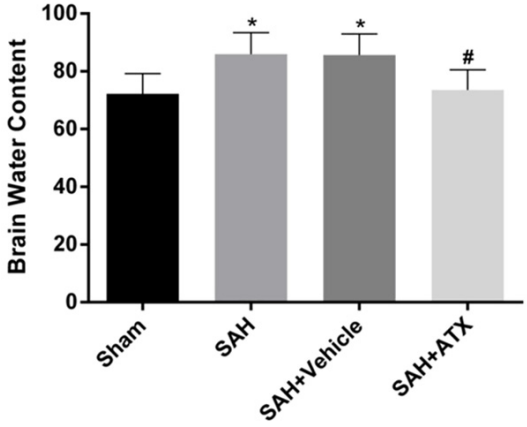

Figure 2. Brain water content in each group. Compared with sham group, *P<0.05; compared with SAH group, #P<0.05. ATX: astaxanthin; SAH: subarachnoid hemorrhage.

tion solution at 37°C for 60 min and sealed in goat serum at room temperature for 30 min. The slice was first incubated overnight at 4°C with primary antibodies that targeted neuronal nuclei antigen and then were incubated with secondary antibody at room temperature for 1 h. Before adding fluorescence quencher, nuclei were counterstained with DAPI. A high magnification optical microscope was employed to observe cell apoptosis.

Statistical analysis

All data were analyzed by using SPSS 21.0 statistical software. The measurement data were shown as mean ± standard deviation. Comparison between groups was performed by independent-samples t test. Comparison among groups was carried out by one-way analysis of variance, followed by LSD method for pairwise comparison. A *P* value of less than 0.05 indicated a statistically significant difference.

Results

Neurological score in each group

Neurological scores of mice in each group were shown in **Figure 1**. Neurological scores in the other three groups were significantly increased compared with the sham group (P<0.05). Neurological scores between the SAH group and SAH + Vehicle group showed no significant difference (P>0.05). Neurological score in the SAH + ATX group was significantly decreased as compared to the SAH group (P<0.05).

Brain water content comparison

Brain water content in each group was shown in **Figure 2**. Brain water content in the other three groups was significantly higher than that in the sham group. Brain water content between SAH group and SAH + Vehicle group did not show a significant difference (P>0.05). Brain water content in the SAH + ATX group was significantly lower than that in the SAH group (P<0.05).

ROS content in brain tissue

ROS content in brain tissue was shown in **Figure 3**. ROS content in the other three groups was significantly increased compared with the sham group. The SAH group and SAH + Vehicle group did not have a significant difference in ROS content (P>0.05). ROS content in the SAH + ATX group was decreased compared with the SAH group (P<0.05).

Inflammatory factor levels in brain tissue

Inflammatory factor levels in brain tissue were shown in **Figure 4**. TNF-α, IL-6 and IL-17 levels in the other three groups significantly increased compared with sham group, and IL-10 level decreased (all P<0.05). The SAH group and SAH + Vehicle group showed no significant difference in inflammatory factors levels (P>0.05). TNF-α, IL-6 and IL-17 levels in SAH + ATX group

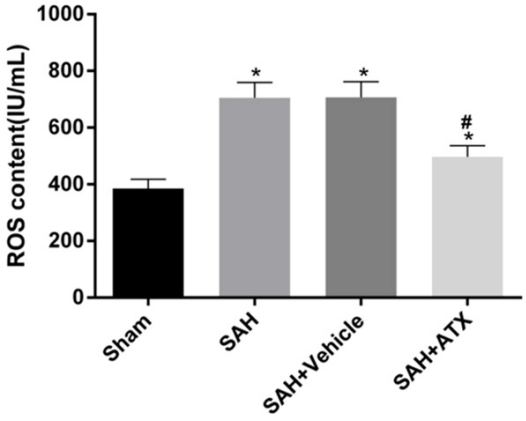

Figure 3. ROS content in brain tissue. Compared with sham group, *P<0.05; compared with SAH group, #P<0.05. ATX: astaxanthin; SAH: subarachnoid hemorrhage; ROS: reactive oxygen species.

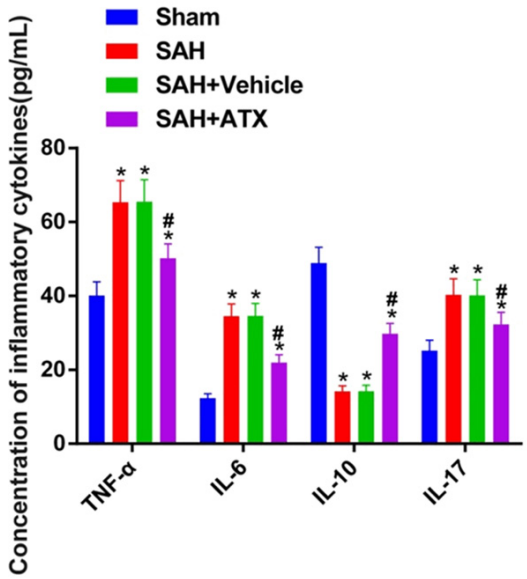

Figure 4. Inflammatory factors levels in brain tissue. Compared with sham group, *P<0.05; compared with SAH group, #P<0.05. ATX: astaxanthin; SAH: subarachnoid hemorrhage; TNF-α: tumor necrosis factor α; IL: interleukin.

decreased, and IL-10 level increased as compared to the SAH group (all P<0.05).

Quantitative real-time polymerase chain reaction and Western blot detection results

Quantitative real-time polymerase chain reaction and Western blot detection results were shown in **Figure 5**. NOX2, GFAP and Bax mRNA and protein expressions in brain tissue of the other three groups were significantly up-regulated compared with the sham group, and Bcl-2 mRNA and protein expressions were significantly down-regulated (all P<0.05). The SAH group and SAH + Vehicle group did not show a significant difference (P>0.05). NOX2, GFAP and Bax mRNA and protein expression in the SAH + ATX group were inhibited compared with the SAH group, and Bcl-2 mRNA and protein expression were up-regulated (all P<0.05).

TUNEL apoptosis detection results

Neuronal apoptosis results in each group were shown in **Figure 6**. Neuronal apoptosis increased in the other three groups compared with the sham group (P<0.05). The SAH group and SAH + Vehicle group did not show a significant difference in neuronal apoptosis (P>0.05). Neuronal apoptosis in the SAH + ATX group was less than that in the SAH group (P<0.05).

Discussion

In this study, we found that ATX significantly relieved the inflammatory response in brain tissue of SAH mice and inhibited neuronal apoptosis. The effect of ATX on SAH might be achieved by regulating inflammatory factor expression and oxidative stress process.

After successful modeling, neurological impairment of mice was scored by Longa scoring method. The results showed that neurological function of mice was impaired after SAH, which could be significantly improved by ATX treatment. The occurrence of SAH could induce the generation of a large number of oxygen free radicals, and the increase of oxygen free radicals further activated the neutrophil pathway, thus damaging the blood-brain barrier, activating related pathways that affected vascular permeability, and causing brain edema [19, 20]. The application of ATX significantly reduced brain water content of SAH mice. In addition, cerebral ischemia and hypoxia after SAH led to a large release of ROS, and high density unsaturated fatty acids that largely existed in nerve tissue were attacked by ROS, aggravating oxidative damage [21-23]. NOX2 is an important member of the NAPDH oxidase family and widely distributed in the central nervous system [24, 25]. A study indicated that NOX2 expression significantly increased after SAH, and inhibiting its expression could significantly improve neurological function of SAH rats and reduce the mortality rate [26]. Another study

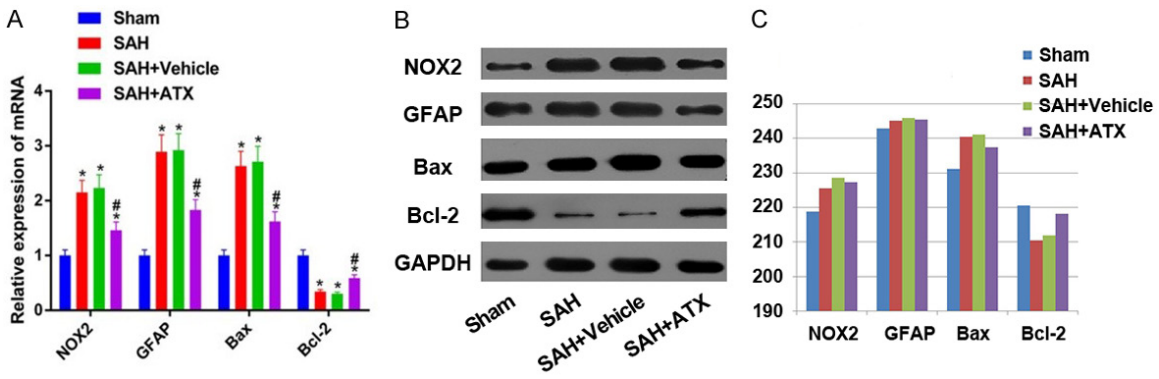

Figure 5. Quantitative real-time polymerase chain reaction and Western blot detection results. A: Relative mRNA expression; B: Protein bands; C: Relative protein expression. Compared with sham group, *P<0.05; compared with SAH group, #P<0.05. ATX: astaxanthin; SAH: subarachnoid hemorrhage; NOX2: NADPH oxidase 2; GFAP: glial fibrillary acidic protein.

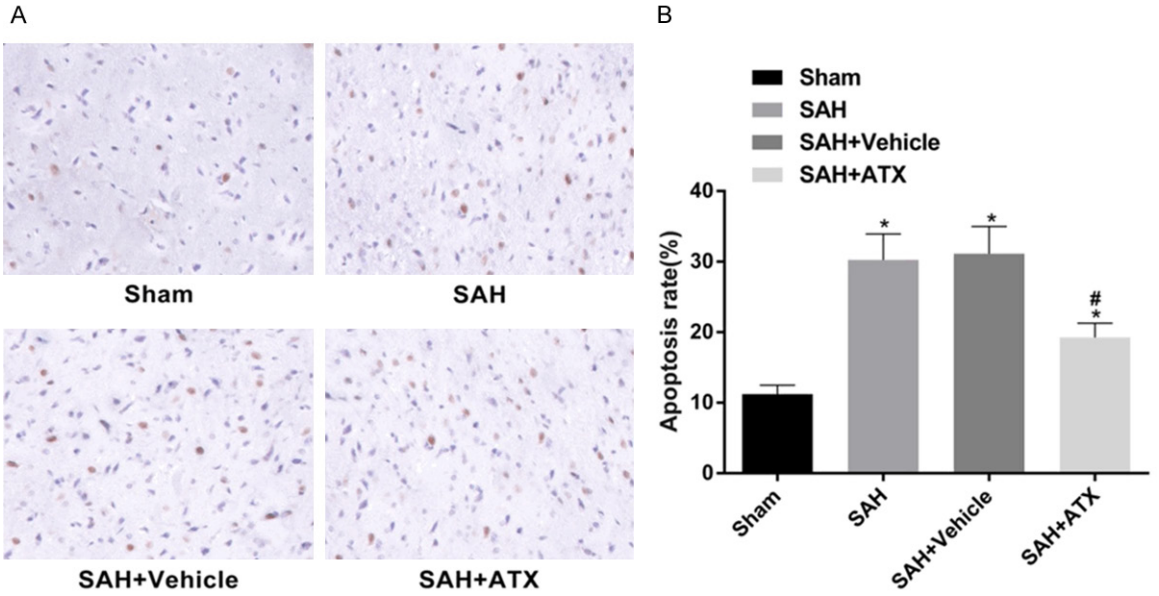

Figure 6. Neuronal apoptosis results in each group. A: TUNEL test results of neurons in each group; B: Apoptosis rate. Compared with sham group, *P<0.05; compared with SAH group, #P<0.05. ATX: astaxanthin; SAH: subarachnoid hemorrhage.

confirmed that NOX2 expression peaked at 12 h after SAH, and a NOX2 inhibitor could significantly improve neurological function of rats and inhibit early neuronal apoptosis [27]. GFAP exists in the gliofibril of astrocytes is the skeleton of astrocytes and is a specific mark protein [28, 29]. GFAP expression increased over time after SAH, indicating that astrocytes were activated unceasingly [30]. In this study, ROS, NOX2 and GFAP expression in brain tissue increased after establishment of SAH mouse models, suggesting that oxidative stress and astrocyte activation in brain tissue is enhanced after SAH, and the action of ATX in SAH was related to its anti-oxidative stress and inhibition of astrocyte activation.

After SAH, macrophages were activated and secreted vast cytokines, including TNF-α, IL-6 and IL-8. It caused the transformation of vascular smooth muscle and further aggravated neuron damage and vascular endothelial cell apoptosis [31, 32]. In this study, TNF-α, IL-6 and IL-17 expressions were significantly enhanced after SAH as compared to sham group, and IL-10 expression was inhibited; the application

of ATX reversed this condition to a certain degree. Meanwhile, ATX could effectively inhibit Bax expression in brain tissue, promote the enhancement of Bcl-2 expression, and reduce neuronal apoptosis that was caused by SAH, thus playing a protective effect in SAH.

In summary, ATX can effectively inhibit oxidative stress and inflammatory response that were caused by SAH, as well as reduce neuronal apoptosis and damage. Therefore, ATX can be a method for the treatment of SAH.

Acknowledgements

This work was supported by the Key Research Development Plan Project of Zhenjiang City-Social Development Project (SH2016042), Six Talents Summit Program of Jiangsu Province (WSW-123) and Hospital-level Project of Zhenjiang First People's Hospital (Y2020009).

Disclosure of conflict of interest

None.

Address correspondence to: Junfei Shao, Department of Neurosurgery, Nanjing Medical University Affiliated Wuxi People's Hospital, No. 299 Qingyang Road, Wuxi 214023, Jiangsu Province, China. Tel: +86-0510-82700775; Fax: +86-0510-82700775; E-mail: wxbrain@163.com

References

[1] Lawton MT and Vates GE. Subarachnoid hemorrhage. N Engl J Med 2017; 377: 257-266.

[2] Schneider UC, Davids AM, Brandenburg S, Muller A, Elke A, Magrini S, Atangana E, Turkowski K, Finger T, Gutenberg A, Gehlhaar C, Bruck W, Heppner FL and Vajkoczy P. Microglia inflict delayed brain injury after subarachnoid hemorrhage. Acta Neuropathol 2015; 130: 215-231.

[3] Abraham MK and Chang WW. Subarachnoid Hemorrhage. Emerg Med Clin North Am 2016; 34: 901-916.

[4] Dubosh NM and Edlow JA. Diagnosis of subarachnoid hemorrhage: time for a paradigm shift? Acad Emerg Med 2017; 24: 1514-1516.

[5] Xia DY, Zhang HS, Wu LY, Zhang XS, Zhou ML and Hang CH. Pentoxifylline alleviates early brain injury after experimental subarachnoid hemorrhage in rats: possibly via inhibiting TLR 4/NF-kappaB signaling pathway. Neurochem Res 2017; 42: 963-974.

[6] Pluta RM, Hansen-Schwartz J, Dreier J, Vajkoczy P, Macdonald RL, Nishizawa S, Kasuya H, Wellman G, Keller E, Zauner A, Dorsch N, Clark J, Ono S, Kiris T, Leroux P and Zhang JH. Cerebral vasospasm following subarachnoid hemorrhage: time for a new world of thought. Neurol Res 2009; 31: 151-158.

[7] Xu T, Zhang WG, Sun J, Zhang Y, Lu JF, Han HB, Zhou CM and Yan JH. Protective effects of thrombomodulin on microvascular permeability after subarachnoid hemorrhage in mouse model. Neuroscience 2015; 299: 18-27.

[8] Wu W, Guan Y, Zhao G, Fu XJ, Guo TZ, Liu YT, Ren XL, Wang W, Liu HR and Li YQ. Elevated IL-6 and TNF-alpha levels in cerebrospinal fluid of subarachnoid hemorrhage patients. Mol Neurobiol 2016; 53: 3277-3285.

[9] Sharma K, Sharma D, Sharma M, Sharma N, Bidve P, Prajapati N, Kalia K and Tiwari V. Astaxanthin ameliorates behavioral and biochemical alterations in in-vitro and in-vivo model of neuropathic pain. Neurosci Lett 2018; 674: 162-170.

[10] Zhang H, Yang W, Li Y, Hu L, Dai Y, Chen J, Xu S, Xu X and Jiang H. Astaxanthin ameliorates cerulein-induced acute pancreatitis in mice. Int Immunopharmacol 2018; 56: 18-28.

[11] Balci Yuce H, Lektemur Alpan A, Gevrek F and Toker H. Investigation of the effect of astaxanthin on alveolar bone loss in experimental periodontitis. J Periodontal Res 2018; 53: 131-138.

[12] El-Agamy SE, Abdel-Aziz AK, Wahdan S, Esmat A and Azab SS. Astaxanthin ameliorates doxorubicin-induced cognitive impairment (chemobrain) in experimental rat model: impact on oxidative, inflammatory, and apoptotic machineries. Mol Neurobiol 2018; 55: 5727-5740.

[13] Kim B, Farruggia C, Ku CS, Pham TX, Yang Y, Bae M, Wegner CJ, Farrell NJ, Harness E, Park YK, Koo SI and Lee JY. Astaxanthin inhibits inflammation and fibrosis in the liver and adipose tissue of mouse models of diet-induced obesity and nonalcoholic steatohepatitis. J Nutr Biochem 2017; 43: 27-35.

[14] Xue XL, Han XD, Li Y, Chu XF, Miao WM, Zhang JL and Fan SJ. Astaxanthin attenuates total body irradiation-induced hematopoietic system injury in mice via inhibition of oxidative stress and apoptosis. Stem Cell Res Ther 2017; 8: 7.

[15] Nai Y, Liu H, Bi X, Gao H and Ren C. Protective effect of astaxanthin on acute cerebral infarction in rats. Hum Exp Toxicol 2018; 37: 929-936.

[16] Pan L, Zhou Y, Li XF, Wan QJ and Yu LH. Preventive treatment of astaxanthin provides neuroprotection through suppression of reactive oxygen species and activation of antioxidant defense pathway after stroke in rats. Brain Res Bull 2017; 130: 211-220.

[17] Lin TY, Lu CW and Wang SJ. Astaxanthin inhibits its glutamate release in rat cerebral cortex nerve terminals via suppression of voltage-dependent Ca(2+) entry and mitogen-activated protein kinase signaling pathway. J Agric Food Chem 2010; 58: 8271-8278.

[18] Longa EZ, Weinstein PR, Carlson S and Cummins R. Reversible middle cerebral artery occlusion without craniectomy in rats. Stroke 1989; 20: 84-91.

[19] Savarraj J, Parsha K, Hergenroeder G, Ahn S, Chang TR, Kim DH and Choi HA. Early brain injury associated with systemic inflammation after subarachnoid hemorrhage. Neurocrit Care 2018; 28: 203-211.

[20] Claassen J, Carhuapoma JR, Kreiter KT, Du EY, Connolly ES and Mayer SA. Global cerebral edema after subarachnoid hemorrhage: frequency, predictors, and impact on outcome. Stroke 2002; 33: 1225-1232.

[21] Yang S, Chen X, Li S, Sun B and Hang C. Melatonin treatment regulates SIRT3 expression in early brain injury (EBI) due to reactive oxygen species (ROS) in a mouse model of subarachnoid hemorrhage (SAH). Med Sci Monit 2018; 24: 3804-3814.

[22] Li X, Zhao L, Yue L, Liu H, Yang X, Wang X, Lin Y and Qu Y. Evidence for the protective effects of curcumin against oxyhemoglobin-induced injury in rat cortical neurons. Brain Res Bull 2016; 120: 34-40.

[23] Li J, Chen J, Mo H, Chen J, Qian C, Yan F, Gu C, Hu Q, Wang L and Chen G. Minocycline protects against NLRP3 inflammasome-induced inflammation and P53-associated apoptosis in early brain injury after subarachnoid hemorrhage. Mol Neurobiol 2016; 53: 2668-2678.

[24] Liu H, Zhao L, Yue L, Wang B, Li X, Guo H, Ma Y, Yao C, Gao L, Deng J, Li L, Feng D and Qu Y. Pterostilbene attenuates early brain injury following subarachnoid hemorrhage via inhibition of the NLRP3 inflammasome and Nox2-related oxidative stress. Mol Neurobiol 2017; 54: 5928-5940.

[25] Pang J, Peng J, Matei N, Yang P, Kuai L, Wu Y, Chen L, Vitek MP, Li F, Sun X, Zhang JH and Jiang Y. Apolipoprotein E exerts a whole-brain protective property by promoting M1? Microglia quiescence after experimental subarachnoid hemorrhage in mice. Transl Stroke Res 2018; 9: 654-668.

[26] Ostrowski RP, Tang J and Zhang JH. Hyperbaric oxygen suppresses NADPH oxidase in a rat subarachnoid hemorrhage model. Stroke 2006; 37: 1314-1318.

[27] Zhang L, Li Z, Feng D, Shen H, Tian X, Li H, Wang Z and Chen G. Involvement of Nox2 and Nox4 NADPH oxidases in early brain injury after subarachnoid hemorrhage. Free Radic Res 2017; 51: 316-328.

[28] Ciccarelli R, D'Alimonte I, Santavenere C, D'Auro M, Ballerini P, Nargi E, Buccella S, Nicosia S, Folco G, Caciagli F and Di Iorio P. Cysteinyl-leukotrienes are released from astrocytes and increase astrocyte proliferation and glial fibrillary acidic protein via cys-LT1 receptors and mitogen-activated protein kinase pathway. Eur J Neurosci 2004; 20: 1514-1524.

[29] Lei J, Gao G, Feng J, Jin Y, Wang C, Mao Q and Jiang J. Glial fibrillary acidic protein as a biomarker in severe traumatic brain injury patients: a prospective cohort study. Crit Care 2015; 19: 362.

[30] Sabri M, Kawashima A, Ai J and Macdonald RL. Neuronal and astrocytic apoptosis after subarachnoid hemorrhage: a possible cause for poor prognosis. Brain Res 2008; 1238: 163-171.

[31] Xu H, Li J, Wang Z, Feng M, Shen Y, Cao S, Li T, Peng Y, Fan L, Chen J, Gu C, Yan F, Wang L and Chen G. Methylene blue attenuates neuroinflammation after subarachnoid hemorrhage in rats through the Akt/GSK-3beta/MEF2D signaling pathway. Brain Behav Immun 2017; 65: 125-139.

[32] Peng Y, Jin J, Fan L, Xu H, He P, Li J, Chen T, Ruan W and Chen G. Rolipram attenuates early brain injury following experimental subarachnoid hemorrhage in rats: possibly via regulating the SIRT1/NF-kappaB pathway. Neurochem Res 2018; 43: 785-795.